A Unified Approach to Driver Assistance Systems Based on Artificial Potential Fields

J. Christian Gerdes

Design Division
Department of Mechanical Engineering
Stanford University
Stanford, California 94305-4021
Email: gerdes@cdr.stanford.edu

Eric J. Rossetter

Design Division
Department of Mechanical Engineering
Stanford University
Stanford, California 94305-4021
Email: ejross@cdr.stanford.edu

Abstract

This paper presents an approach to vehicle control based on the paradigm of artificial potential fields. Using this method, the dynamics of the vehicle are coupled with the environment in a manner that ensures that the system exhibits safe motion in the absence of driver inputs. The driver remains in control of the vehicle, however, with the control systems presenting a predictable and safe set of dynamics. With the control approach presented here, integration of various assistance systems is easily achieved through simple superposition of individual potential and damping functions. A simple example of a combined lanekeeping and stability system demonstrates how this can be accomplished. Preliminary simulation results suggest that both safety and driveability are achievable with such a system, prompting further investigation.

1 Introduction

While anti-lock brake systems designed to prevent wheel lock-up are now common and stability control programs designed to prevent skidding are seeing increased popularity, responsibility for avoiding collisions with objects in the environment remains solely with the driver. Though humans are quite adept at this task, they are far from infallible; in 1996, for instance, the first harmful event for 28.9% of fatal crashes was a collision with a fixed object in the environment (NHTSA [1]). The work presented here envisions vehicle control as a means of fundamentally altering these dynamic relationships to enable the driver to operate in a nominally safe vehicle/environment system. Instead of viewing driver assistance as a collection of individual functions, we view it as a redesign of the driving experience. Ultimately, a successful redesign should make this experience safer, more fun and tunable to individual driving styles or preferences.

The paradigm chosen for this new relationship is that of an artificial potential field. First proposed by Khatib [2] for robotic manipulator control and by Hogan [3] in the general context of impedance control, potential fields have seen considerable application to obstacle avoidance and mobile robots. There have also been several applications of potential fields or impedance to the control of passenger cars and heavy trucks. Reichhardt and Schick [4] proposed an electric field interpretation for autonomous vehicle control based upon a risk map. The risk map assigned a value corresponding to the relative hazard to every point in a two-dimensional description of space. This hazard at each point, interpreted as a charge, exerted a force on the vehicle (interpreted as an electron) with the resultant force from all charges in the environment determining the path

of the autonomous vehicle. Since the vehicle dynamics were not considered, it was assumed that the vehicle could in fact track this trajectory. Reichardt [5] later merged lanekeeping, obstacle avoidance and traffic sign recognition into the construction of the risk map. Hennessey *et al.* [6] used a spring analogy to define "virtual bumpers" in 2D collision avoidance strategies, in effect attaching an impedance or potential field to the vehicle. This controller was coupled with a heuristic lane change control for collision avoidance (Schiller *et al.* [7]) and demonstrated on an autonomous land vehicle (Schiller *et al.* [8]). Like the work of Reichardt and Schick [4], these results did not explicitly incorporate the vehicle dynamics.

In this paper, we propose an interpretation of driver assistance systems as potential fields and generalized damping functions added to the existing vehicle dynamics and driver inputs. Viewed within the language of impedance control (Hogan [3]), the potential fields and damping turn the environment into an impedance, providing restoring forces which move the vehicle towards safer regions of the state space. The controller does not attempt to interpret driver intent, but merely presents a safe, predictable dynamic response to the driver. Leaving the inherent dynamics in place is a novel approach to creating a driveable system and enables the assistance systems to smoothly enter and leave the dynamics as needed. By leaving the driver in the loop, high-level tasks such as path planning remain the province of the driver, thereby avoiding the difficulties of local minima which can arise with potential field controllers. This local nature of the control design allows the system to use a local representation of the environment, avoiding the computational difficulties noted by Reichardt and Schick [4].

This paper outlines the basic approach and presents a proof of the nominally safe behavior provided by the system. To illustrate the application of these ideas, a combined lanekeeping and yaw control application is presented. Because of the superposition property of the controller, a potential field description of lanekeeping and the damping interpretation of yaw control can simply be added together to produce a system with nominally safe behavior. While it is easily established that the new system has nominally safe dynamics, performance and driver acceptance are not clear. To examine these issues, simulations of vehicle performance in a lane change maneuver are presented. The results suggest that a driver can intuitively drive in the potential field framework and integration of various control functions can be achieved in the proposed manner. A brief summary of the future directions suggested by these preliminary results concludes the paper.

2 Basic Approach

Robotic control using artificial potential fields was originally motivated by the desire to move some of the responsibility for collision avoidance from a high-level (and consequently slow) planning task to the lowest (and fastest) level of control (Khatib [2]). By directly coupling sensing to certain types of actuation, fast environmental hazards could be handled instinctively, rather than by high-level planning. This analogy transfers well to driver assistance systems. By keeping the driver in the loop, human capacity for high-level planning remains central to the driving experience while advanced control systems provide added convenience or faster response to hazards.

The unifying principle behind this approach is to consider each vehicle control system as assessing some penalty, or level of hazard, on different regions of the state space. The potential function is determined by summing the hazard assessed by each system on the position variables. The damping function, in turn, penalizes velocity variables. The controller (or controllers, when multiple systems are involved) then provides a level of restoring force corresponding to the gradient of the potential function (referred to as the potential field) along with the artificial damping. The vehicle therefore exhibits a natural tendency to return to areas of the state space with low levels

of hazard, assisting the driver with low-level control tasks. With this approach, sensor fusion is captured systematically by the creation of the potential and damping functions and coordination among different actuators is embodied in the generation of the restoring force.

The following examples serve to better explain this concept of an artificial potential field defined by degree of hazard. Figure 1 illustrates a cross section of the environmental hazards seen by the car in the right lane in the manner envisioned by Reichardt [5]. Should the driver drift so that lane departure or a collision with the other vehicle becomes likely, the potential hazard would increase and the controller would provide a greater restoring force to move the vehicle to a safer region (in this case, the center of its lane). Interactions among safety and convenience systems can be easily viewed in such a context. For example, knowledge of the road curvature may allow a car's on-center feel to be associated with proper lane tracking as opposed to straight-line motion.

Expressing driver assistance systems in terms of potential and damping functions offers several insights. First, since artificial potential fields represent a complete redesign of the dynamic relationship between a system and its environment, this view opens up new possibilities for design of the driving experience. One extremely simple example of this is relating on-center feel to lane tracking, as previously mentioned. Second, the superposition property of potential functions allows for better analysis and design of interactions among control systems. This is especially true for interactions between systems that react primarily to environmental stimuli (like collision avoidance or lanekeeping) and those which react primarily to the vehicle state (such as stability control). While such systems have been developed separately, it is not hard to envision interactions involving, for instance, a choice between skidding and lane departure (this is particularly true if the scope is extended to heavy trucks with multiple trailers). Third, the level of assistance provided can be adjusted by simple scaling of the potential function. Increasing the "height" of the potential function peaks relative to the valleys creates a greater restoring force in response to a given hazard, thus providing a higher level of assistance (or intrusiveness).

2.1 Vehicle and Environment Models

The vehicle model used in this study (Figure 2) is a simple yaw plane representation with three degrees of freedom (Koepele and Starkey [9]) and differential braking capability:

$$m\dot{U}_x = [F_{xr} + F_{xf}\cos\delta - F_{yf}\sin\delta + mrU_y] \tag{1}$$

$$m\dot{U}_y = [F_{yr} + F_{xf}\sin\delta + F_{yf}\cos\delta - mrU_x] \tag{2}$$

$$I_z\dot{r} = \left[aF_{xf}\sin\delta + aF_{yf}\cos\delta - bF_{yr} + \Delta F_{xr}\frac{d}{2} + \Delta F_{xf}\frac{d}{2}\cos\delta\right] \tag{3}$$

where

$$F_{xf} = F_{xrf} + F_{xlf} \tag{4}$$

$$F_{xr} = F_{xrr} + F_{xlr} \tag{5}$$

$$\Delta F_{xf} = F_{xrf} - F_{xlf} \tag{6}$$

$$\Delta F_{xr} = F_{xrr} - F_{xlr} \tag{7}$$

While the double-track model is used for the purposes of differential braking, we assume that the left and right tires possess the same slip angle (in other words, using a simple bicycle model for the kinematics). Assuming a vehicle with throttle-, brake- and steer-by-wire capability, the longitudinal forces and steer angle can be controlled so the equations of motion can be rewritten as

$$D\ddot{q} = f(\dot{q}) + g(\dot{q}, u_c) \tag{8}$$

where the velocity and control vectors are defined as

$$\dot{q} = [U_x\ U_y\ r]^T \tag{9}$$
$$u_c = [\delta\ F_{xrf}\ F_{xlf}\ F_{xrr}\ F_{xlr}]^T \tag{10}$$

The vectors f and g are described by

$$f = \begin{bmatrix} mrU_y \\ F_{yr} - mrU_x + \hat{F}_{yf} \\ -bF_{yr} + a\hat{F}_{yf} \end{bmatrix} \tag{11}$$

$$g = \begin{bmatrix} F_{xr} + F_{xf}\cos\delta - F_{yf}\sin\delta \\ F_{xf}\sin\delta + F_{yf}\cos\delta - \hat{F}_{yf} \\ aF_{xf}\sin\delta + aF_{yf}\cos\delta - a\hat{F}_{yf} + \Delta F_{xr}\frac{d}{2} + \Delta F_{xf}\frac{d}{2}\cos\delta \end{bmatrix} \tag{12}$$

where

$$\hat{F}_{yf} = -\hat{C}_f\left(\frac{ra + U_y}{U_x}\right)\ sgn(U_x) \tag{13}$$

for some effective cornering stiffness, $\hat{C}_f \geq 0$. This separates the dynamics into a drift vector depending only on $\dot{q}$ and a control vector involving components of u_c. The *sgn* term is added to account for the sign change when $U_x < 0$, which is lost in the small angle approximation. It is unlikely, but possible to have a negative U_x in emergency situations such as an uncontrolled spin. This linear definition for tire force is, however, undefined at $U_x = 0$.

The inclusion of the term $\hat{F}_{yf}$ can be motivated as follows. Geometrically, the front and rear slip angles are described by:

$$\alpha_f = \tan^{-1}\left(\frac{ra + U_y}{U_x}\right) - \delta \tag{14}$$
$$\alpha_r = \tan^{-1}\left(\frac{U_y - rb}{U_x}\right) \tag{15}$$

As a first approximation, the lateral force of a tire can be approximated as a linear function of the slip angle

$$F_{yf} = -\hat{C}_f\alpha_f \tag{16}$$

where $\hat{C}_f$ is the effective cornering stiffness of the tire ("effective" since it may involve modification for combined slip characteristics as described in Section 2.3). Using small angle assumptions,

$$F_{yf}\cos\delta \approx -\hat{C}_f\left(\frac{ra + U_y}{U_x}\right) + \hat{C}_f\delta \tag{17}$$

$\hat{F}_{yf}$ thus represents an approximation to the part of the tire force that does not include the steering angle δ. With $\hat{F}_{yf}$, therefore, the portion of the nonlinear term $F_{yf}\cos\delta$ that does not include a control input is properly assigned to the drift vector, at least approximately.

Using this definition, the drift term f is a dissipative term due to the inherent energy dissipation of the tires. Under the assumption that the tire force and the slip angle are oppositely directed,

$$\begin{aligned} \dot{q}^T f &= F_{yr}(U_y - br) + \hat{F}_{yf}(U_y + ra) \\ &= F_{yr}(U_y - br) - \hat{C}_f\frac{(U_y + ra)^2}{|U_x|} \\ &\leq 0 \end{aligned}$$

This damping characteristic of tires was demonstrated using a linear model by Chen and Tomizuka [10] and Gerdes and Rossetter [11]. The treatment here underscores that this observation is not a result of linearization, but rather follows from the basic physics of the problem. The key idea is that the tire force acts in a direction opposite that of the slip angle that produces it (which, with the possibility of a slight offset, must be true given the mechanisms of deformation and friction that produce tire forces). While a specific tire model is necessary for implementation (Section 2.3), the damping nature of the drift term is independent of model choice. The damping nature of the drift vector plays an important role in the formulation of the control law: since this term always results in a net loss of energy from the system, cancellation of these dynamics is not necessary to avoid environmental hazards.

For this paper, the environment is modeled simply as a straight section of roadway with the position vector $w = [s\ e\ \psi]^T$ representing the distance down the roadway, the lateral offset, and the heading angle, respectively (Figure 3). The state vector of the system is therefore given in terms of the position variables, w and the velocity vector $\dot{q}$. Transformation between the environmental and body fixed systems can be achieved through:

$$\frac{\partial \dot{w}}{\partial \dot{q}} = \frac{\partial w}{\partial q} = \begin{bmatrix} \cos\psi & -\sin\psi & 0 \\ \sin\psi & \cos\psi & 0 \\ 0 & 0 & 1 \end{bmatrix} \tag{18}$$

2.2 Control Law

With the assumption of throttle-, brake- and steer-by-wire, the control vector u_c must combine commands from the driver and the assistance system. The control vector must therefore solve

$$g(\dot{q}, u_c) = B_d(\dot{q}, u_d) + F(w, \dot{q}, u_d) - \left(\frac{\partial V}{\partial w}\frac{\partial w}{\partial q}\right)^T \tag{19}$$

where $B_d(\dot{q}, u_d)$ is the portion corresponding to the driver input and the remaining two terms come from the assistance system. $V(w)$ is the potential function describing the overall hazard in the environment and $F(w, \dot{q}, u_d)$ is a generalized damping term. This term can be any vector function that satisfies

$$\dot{q}^T F(w, \dot{q}, u_d) \leq 0 \tag{20}$$

The driver commands, u_d, consist of the steering wheel, δ_d, the accelerator pedal, F_{ad}, and the brake pedal, F_{bd}. The complete driver command vector is

$$u_d = [\delta_d\ F_{ad}\ F_{bd}]^T \tag{21}$$

If we set

$$B_d(\dot{q}, u_d) \doteq g(\dot{q}, \begin{bmatrix} \delta_d \\ -\frac{F_{bd}}{4} \\ -\frac{F_{bd}}{4} \\ \frac{F_{ad}}{2} - \frac{F_{bd}}{4} \\ \frac{F_{ad}}{2} - \frac{F_{bd}}{4} \end{bmatrix}) \tag{22}$$

then the vehicle will respond to driver inputs as if it had rear-wheel drive and standard connections (ignoring brake proportioning). With full x-by-wire capability, other mappings from driver inputs to control inputs are possible but this represents the simplest choice.

With a differentiable potential function, $V(w)$, and a damping function that satisfies Equation 20, the system will exhibit a nominally safe behavior.

Proposition 2.1 (Nominally Safe Behavior) *If the potential function $V(w)$ is interpreted as a level of hazard applied to system states, then in the absence of driver input, the system hazard is bounded by:*

$$V_{max} = \frac{1}{2}\dot{q}(0)^T D\dot{q}(0) + V(w(0))$$

where $w(0)$ and $\dot{q}(0)$ are the values at the initial time $t = 0$.

Proof Defining an effective energy as the sum of the vehicle's kinetic energy and the artificial potential energy from the potential field yields:

$$E = \frac{1}{2}\dot{q}^T D\dot{q} + V(w)$$

The rate of change of energy is:

$$\begin{aligned}
\dot{E} &= \dot{q}^T D\ddot{q} + \frac{\partial V}{\partial w}\frac{\partial w}{\partial q}\dot{q} \\
&= \dot{q}^T \left[f(\dot{q}) + g(\dot{q}, u_c)\right] + \frac{\partial V}{\partial w}\frac{\partial w}{\partial q}\dot{q} \\
&= \dot{q}^T \left[f(\dot{q}) + B_d(\dot{q}, 0) + F(\dot{q}, w, 0) - \left(\frac{\partial V}{\partial w}\frac{\partial w}{\partial q}\right)^T\right] + \frac{\partial V}{\partial w}\frac{\partial w}{\partial q}\dot{q} \\
&= \dot{q}^T \left[f(\dot{q}) + F(\dot{q}, w, 0) - \left(\frac{\partial V}{\partial w}\frac{\partial w}{\partial q}\right)^T\right] + \frac{\partial V}{\partial w}\frac{\partial w}{\partial q}\dot{q} \\
&= \dot{q}^T f(\dot{q}) + \dot{q}^T F(w, \dot{q}, 0) \\
&\leq 0
\end{aligned}$$

Since the effective energy cannot increase

$$V_{max} \leq E_0 = \frac{1}{2}\dot{q}(0)^T D\dot{q}(0) + V(w(0))$$

bounds the hazard experienced by the system.

2.3 Solving for the Control Inputs

The previous proof requires that the individual control inputs, u_c, produce a control vector, $g(\dot{q}, u_c)$, that satisfies Equation 19. Solving for an appropriate choice of inputs, in turn, requires the use of a specific tire model. In contrast to the linear model used by Gerdes and Rossetter [11], the following solution for the control vector uses a simplified version of the Dugoff tire model (Guntur and Sankar [12]) in order to capture the coupling between lateral and longitudinal forces. These forces can be specified at each tire in terms of the longitudinal tire slip, s, slip angle, α, normal force, F_n, and friction coefficient, μ:

$$F_x = -\frac{C_x s}{1-s} f(\lambda) \tag{23}$$

$$F_y = -\frac{C_y \tan\alpha}{1-s} f(\lambda) \tag{24}$$

where,

$$\lambda = \frac{\mu F_n (1-s)}{2[(C_x s)^2 + (C_y tan\alpha)^2]^{1/2}} \tag{25}$$

and

$$f(\lambda) = \begin{cases} (2-\lambda)\lambda & : \quad \lambda < 1 \\ 1 & : \quad \lambda \geq 1 \end{cases} \tag{26}$$

For simplicity in solving for the control vector, it is assumed in this paper that the tires are not near saturation. In this region, the non-linear $f(\lambda)$ term equals one. If saturation is taken into account, a solution for u_c can be found using iterative techniques on the procedure presented below. To get F_y in terms of the control inputs the slip term has to be eliminated. Assuming a static representation of slip, the longitudinal force equation can be solved to give:

$$s = \frac{F_x}{F_x - C_x} \tag{27}$$

Substituting this expression into F_y and assuming small angles gives the following expression for the front lateral force:

$$F_{yf} = C_{yf}\delta - C_{yf}(\frac{ra + U_y}{U_x}) - \frac{C_{yf}}{C_{xf}}F_{xf}\delta + \frac{C_{yf}}{C_{xf}}F_{xf}(\frac{ra + U_y}{U_x}) \tag{28}$$

This equation for F_{yf} is substituted into Equation 12 to obtain an expression that is solely in terms of the control vector u_c.

$$g(\dot{q}, u_c) \quad = \quad \begin{bmatrix} F_{xf} - (C_{yf}\delta - C_{yf}(\frac{ra+U_y}{U_x}) - \frac{C_{yf}}{C_{xf}}F_{xf}\delta + \frac{C_{yf}}{C_{xf}}F_{xf}(\frac{ra+U_y}{U_x}))\delta + F_{xr} \\ F_{xf}\delta + C_{yf}\delta - \frac{C_{yf}}{C_{xf}}F_{xf}\delta + \frac{C_{yf}}{C_{xf}}F_{xf}(\frac{ra+U_y}{U_x}) \\ (\Delta F_{xr} + \Delta F_{xf})\frac{d}{2} + F_{xf}\delta a + (C_{yf}\delta - \frac{C_{yf}}{C_{xf}}F_{xf}\delta + \frac{C_{yf}}{C_{xf}}F_{xf}(\frac{ra+U_y}{U_x}))a \end{bmatrix} \tag{29}$$

To solve for u_c, the above vector equation is set equal to the generalized force terms of Equation 19. Solving for the controlled terms involves manipulation of each equation in the control vector. Therefore, the following notation is introduced to separate Equation 19 into the desired force components and equate the terms with those in Equation 29.

$$\begin{bmatrix} g_{des}(1) \\ g_{des}(2) \\ g_{des}(3) \end{bmatrix} = B_d(\dot{q}, u_d) + F(w, \dot{q}, u_d) - \left(\frac{\partial V}{\partial w}\frac{\partial w}{\partial q}\right)^T \tag{30}$$

The controlled dynamics of Equation 29 are set equal to the above force components to solve for the control vector u_c.

$$F_{xf} - (C_{yf}\delta - C_{yf}(\frac{ra + U_y}{U_x}) - \frac{C_{yf}}{C_{xf}}F_{xf}\delta + \frac{C_{yf}}{C_{xf}}F_{xf}(\frac{ra + U_y}{U_x}))\delta + F_{xr} = g_{des}(1) \tag{31}$$

$$F_{xf}\delta + C_{yf}\delta - \frac{C_{yf}}{C_{xf}}F_{xf}\delta + \frac{C_{yf}}{C_{xf}}F_{xf}(\frac{ra + U_y}{U_x}) = g_{des}(2) \tag{32}$$

$$(\Delta F_{xr} + \Delta F_{xf})\frac{d}{2} + F_{xf}\delta a + (C_{yf}\delta - \frac{C_{yf}}{C_{xf}}F_{xf}\delta + \frac{C_{yf}}{C_{xf}}F_{xf}(\frac{ra + U_y}{U_x}))a = g_{des}(3) \tag{33}$$

Since this system is underdetermined, two extra constraints are added in order to solve for the control vector u_c. The first constraint is to assume a differential braking distribution, which is given in Figure 4. This distribution puts all the differential braking on the front wheels until a magnitude of 500 N is reached. If the total differential braking required is above this amount, the extra force is distributed evenly between the front and rear wheels. The value for switching

some of the differential load to the rear was chosen based on the lowest coefficient of friction used in the simulation. In reality, this value could be based on results from μ estimation. The second constraint, shown in Figure 5, distributes the total braking between front and rear. Since we are assuming a rear wheel drive vehicle, the front wheels can only provide braking forces. The minimum amount of braking force is determined by the differential braking needed at the front. Therefore, if the vehicle needs a total force that is larger than the braking force at the front, this must come from the rear wheels. If the total force is less than the minimum front braking force, the extra braking force required is evenly distributed between the front and rear of the vehicle.

To solve for the control inputs, Equation 33 is subtracted from Equation 32 multiplied by the parameter a. This gives an expression for the total differential braking needed in the system:

$$\Delta F_{x\_total} = \Delta F_{xr} + \Delta F_{xf} = -\frac{2}{d}(a g_{des}(2) - g_{des}(3)) \tag{34}$$

Using the first constraint in Figure 4, the differential braking at the front and rear can be determined.

The total longitudinal force required is estimated by neglecting terms involving δ from Equation 31.

$$F_{xf} + F_{xr} = g_{des}(1) \tag{35}$$

Using this estimate, the total force at the front can be determined from the second constraint in Figure 5. This value for F_{xf} is substituted into Equation 32 and the steering angle, δ, can be found. The steering angle and front longitudinal force are then used in Equation 31 to solve for the total rear longitudinal force, F_{xr}. With the total and differential longitudinal forces now known for each axle, the longitudinal force at each wheel can be determined.

3 A Lanekeeping and Yaw Control System

To demonstrate the coupling of environmental and vehicle states in this paradigm, we consider the simple example of a combined lanekeeping and stability control system. This example is intended to highlight some of the functionality that can be achieved by simply adding a potential field and generalized damping to the vehicle dynamics; it is not intended to represent an ideal choice of parameters for either system. Indeed, in this paper, lanekeeping is achieved solely through the potential field while stability control functionality follows from the damping term alone. As noted later, coupling may be desirable.

3.1 Potential Field Design

As we have formulated the problem, it is not hard to develop the control law or to guarantee that the system tends to move towards "safer" states (as defined by the potential function) in the absence of driver inputs. In a vehicle system, some other criteria can be formulated:

- The hazards defined by the potential fields between lanes should be calibrated in such a way to prevent lane crossing in the presence of disturbances in the absence of driver inputs.
- The dynamics in the center of the lane should be those of the uncontrolled vehicle.
- The driver should be able to change lanes in a manner qualitatively similar to the uncontrolled system.

The first two can be met analytically in the development of the potential fields. The third is evaluated through simulation with a simple driver model. It is important to keep in mind that this approach to driver assistance does not treat driver inputs as disturbances, rather it simply adds control commands to move the vehicle states to a "safer" region. The driver can choose to ignore the effects of these control inputs through his or her control authority (much like maintaining the lane in the presence of a sidewind or banked road). The potential field will affect a driver's response, but this should be minimal in cases such as changing lanes. The potential function chosen for the lanekeeping task is solely a function of lateral error, e, and is illustrated in Figure 6. This corresponds to a highway with two lanes traveling in the same direction and lane centers at $e = 0m$ and $e = 3.5m$. For information on the position in the lane and lane curvature, we assume either the use of a GPS system coupled with a precision map (Wilson *et al.* [13]), or a vision system that references lane markings (Gehrig and Stein [14]). The potential function is much greater for road departure than for lane crossing, consistent with intuition.

Several constraints on the potential function are required to produce an appropriate design. First, the potential function is flat in the center of the lane to give the driver the opportunity to maneuver without intrusion. Second, the gradient is zero at the point exactly between the lane centers (1.75 m) to prevent a discontinuous change in the system dynamics at this point. Finally, the peak value of the field in each section is scaled to correspond to the energy required to overcome the field.

Generally speaking, there are two critical parameters to consider in the potential function. One is the energy or height of the function and the other is the function's maximum slope. In order to avoid a "hazardous" object, the potential function must be able to store at least the kinetic energy of the system which lies along the gradient of the function. This specifies the height of the potential function. Achieving this height in a given distance (i.e. from the vehicle's current location to the object), places a lower bound on the slope of the function. Since the slope of the potential function corresponds to the control force required by the vehicle, tire saturation places an upper bound on the slope. Therefore, it is crucial to balance the slope of the potential field between the safety requirements and the saturation limits of the vehicle. Ensuring a measure of safety when saturation is unavoidable is the subject of future work.

3.2 Choice of Damping Values

To achieve a stability control function, we would like to be able to alter the vehicle's yaw rate when we sense that it is different from that commanded by the driver. Based upon steady handling results, we define the desired yaw rate in terms of the driver's steering command:

$$r_{des} = \frac{U_x}{L + KU_x^2}\delta_d \tag{36}$$

The yaw rate controller used here is simply:

$$M_{yaw,des} = \gamma(r_{des} - r) \tag{37}$$

Figure 7 conceptually divides this controller into six regions, labeled understeer, oversteer and reverse steer. In the oversteer and reverse steer cases, the desired yaw moment always acts in the opposite direction as the yaw rate, making the damping nature of the controller quite clear. In the understeer case, however, the stability controller increases the yaw rate. If we do not compensate for the effect of the differential braking terms on the longitudinal motion, however, the overall system exhibits a damped response.

Therefore, defining the damping function, F by

$$F(w, \dot{q}, u_d) = \begin{bmatrix} -\frac{2}{d}\gamma|r_{des} - r| \\ 0 \\ \gamma(r_{des} - r) \end{bmatrix} \tag{38}$$

$$\dot{q}^T F(w, \dot{q}, u_d) = r\left[\gamma(r_{des} - r)\right] - 2U_x\gamma|r_{des} - r|/d \tag{39}$$

This expression is less than zero whenever the vehicle is operating in the oversteer or reverse steer regions described above or when the vehicle is operating in the understeer region with:

$$|r| \leq \frac{2U_x}{d} \tag{40}$$

Physically, this corresponds to an instantaneous turning radius greater than half of the track width. Cases where the vehicle is understeering the desired yaw rate while achieving a turning radius of less than half of the track are, to say the least, rare. From a mathematical standpoint, the controller can be shut off or the driver command limited under these conditions to guarantee damping; from a practical standpoint, such a modification will not impact the stability control at all.

While omitted here for simplicity, more realistic features for a stability control system can be added in this framework. Among such enhancements are braking of the front wheels, a threshold level of mismatch between r and r_{des} before the system activates and ensuring that the system does not attempt to track values of r_{des} that cannot be achieved under the current friction conditions (Alberti and Babbel [15]). Additional stabilization based upon the vehicle sideslip angle can also be added within this framework, since counteracting sideslip is comparable to damping on U_y.

4 Simulation Evaluation

Although the system presented here is straightforward to design and amenable to analysis, there is no evidence that the resulting dynamics can easily be controlled by a driver. To examine this, we investigated both the response of the system to a disturbance (with no driver input) and the performance in two different lane change maneuvers. The purpose of these simulations is to determine whether or not this approach could handle the conflicting goals of rejecting disturbances while minimally impacting the ability of the driver to change lanes. The simulation model was the same as the model used in the controller design, with the addition of tire saturation (i.e. eliminating the assumption that $f(\lambda) = 1$ in the Dugoff model) and a dynamic calculation of longitudinal wheel slip. Please see Table 1 for further explanation and the numerical values used in this study.

4.1 Disturbance Rejection

Figure 8 shows the system response for lateral step disturbance of 200N applied to the vehicle. This disturbance approximates the force from gravity due to the crown angle on a four lane road (approx. 0.6 degrees) or a side wind. As can be seen from the plot, the vehicle remains within the lane with this disturbance. The trajectory does move close to the lane edge, but it is important to remember that the center potential field is fairly small in order to allow the driver to change lanes. In order to maintain lane composure in the presence of larger disturbances, the field can be increased appropriately to remove the necessary energy. The response shows a very slow oscillation due to the flatness of the potential function in the lane center and the lack of damping in the potential fields. Such an oscillation could easily be corrected by the driver, though damping could also be added to remove energy from the vehicle while it is in the potential field. This choice is ultimately one of driver acceptance.

Parameter or Variable	Symbol	Value
Front Cornering Stiffness	C_{yf}	145,000 N/rad
Rear Cornering Stiffness	C_{yr}	145,000 N/rad
Front Longitudinal Stiffness	C_{xf}	300,000 N
Rear Longitudinal Stiffness	C_{xr}	300,000 N
Wheelbase	l	2.8 m
Distance from c.g. to Front Tire	a	1.37 m
Distance from c.g. to Rear Tire	b	1.43 m
Track width	d	1.5 m
Vehicle mass	m	1860 kg
Moment of Inertia	I_z	3100 kg m^2
Distance Along Roadway (state)	s	-
Lateral Position (state)	e	-
Yaw Angle (state)	ψ	-
Driver Braking Force (driver input)	F_{bd}	-
Driver Acceleration Force (driver input)	F_{ad}	-
Driver Steering Command (driver input)	δ_d	-
Right Differential Braking Force (input)	F_{br}	-
Left Differential Braking Force (input)	F_{bl}	-
Controller Steering Command (input)	δ_c	-

Table 1: Vehicle Parameters, Variables and Inputs

Parameter	Symbol	Value
Gain	K_{drv}	0.035
Time delay	τ_d	0.2 s
Neuromuscular Lag	τ_n	0.2 s
Lead Constant	τ_1	10 s
Lag Constant	τ_2	0 s
Steering Ratio	K_{steer}	19.6

Table 2: Driver Model Parameters

4.2 Lane Change

A simple driver model from Cooke *et al.* [16] with the following transfer function:

$$\frac{\Delta_d(s)}{E_d(s)} = \frac{K_{drv}}{K_{steer}} \left(\frac{\tau_1 s + 1}{\tau_2 s + 1}\right) \left(\frac{1}{\tau_n s + 1}\right) e^{-\tau_d s} \tag{41}$$

where $\Delta_d(s)$ is the Laplace transform of δ_d and $E_d(s)$ is the Laplace transform of the tracking error used by the driver. The tracking error used is $e_d = e + 14\psi$ where e is the lateral offset and ψ is the heading angle, which is multiplied by a preview distance of $14m$. The parameters in Table 2 were used to generate an estimate of the wheel angle needed to follow a desired trajectory. To evaluate the driveability of the controlled system, a sinusoidal lane change trajectory was fed through the driver model at a speed of 20 m/s. Figure 9 compares the lateral position and driver input for the uncontrolled vehicle and the vehicle with potential fields added. The two responses are strikingly similar. This result is very encouraging, suggesting that driving in the potential field

does not require or provoke a substantially different response from the driver (to the extent that the driver model incorporated here reflects a true human response). The trajectory is also quite similar, suggesting that a potential field capable of lanekeeping in the presence of small disturbances is not overly obtrusive in normal driving. One issue not answered by these simulations, however, is whether or not the force generated by the vehicle controller should in some manner be fed back to the driver through the steering wheel.

4.3 Avoidance Maneuver

To analyze the effect of the stability controller, an avoidance maneuver consisting of a double lane change was also examined. Figure 10 shows this maneuver under three sets of conditions. For a high friction road surface corresponding to a dry road, the driver is able to successfully control the vehicle. When the friction is reduced to a peak value $\mu = 0.3$, however, the vehicle spins, as indicated by the relatively constant yaw velocity of approximately -20 deg/s. With the addition of the stability and potential field controller, the driver is again able to execute the avoidance maneuver with even less oscillation than the high μ, uncontrolled case. Comparison with published results (Alberti and Babbel [15]) shows that the controller response is indeed reasonable. As mentioned previously, the stability control here does not represent a production system due to its simplicity (particularly the lack of a term depending on the slip angle); however, it is illustrative of how control objectives can be merged in this paradigm.

5 Conclusions

This paper outlines the rationale for, and a first application of, a unified approach to driver assistance based upon artificial potential fields. Such an approach offers an intuitive means of creating a nominally safe operating environment for the vehicle while keeping the driver in control. A key advantage is the ability to integrate vehicle control systems with the vehicle dynamics through simple addition of potential and damping functions. Early simulation results give encouragement that a balance between nominally safe behavior and driveability can be struck in such a system. Current work includes extension to other vehicle states, moving obstacles, and convenience features such as adaptive cruise control. To study driver acceptance this system will be implemented on a test vehicle that either has complete drive-by-wire system or steering and braking actuators that can add torques and forces on top of the driver's inputs. This is an important step in this work because the success of such a driver assistance system ultimately comes down to the combination of controller performance and driver acceptance.

6 Acknowledgements

The authors would like to thank Nicholas Fiechter, Pat Langley, Franz May, Mark Pendrith, Dirk Reichardt, Seth Rogers, Avshalom Suissa and Chris Wilson of DaimlerChrysler and Ursina Saur of ETH Zurich for their help in refining these ideas.

References

[1] NHTSA. Traffic safety facts 1996. Technical report, National Highway Traffic Safety Administration, 1997.

[2] O. Khatib. Real-time obstacle avoidance for manipulators and mobile robots. *International Journal of Robotics Research*, 5(1):90–98, 1986.

[3] N. Hogan. Impedance control: An approach to manipulation, parts I-III. ASME *Journal of Dynamic Systems, Measurement, and Control*, 107:1–24, March 1985.

[4] D. Reichardt and J. Schick. Collision avoidance in dynamic environments applied to autonomous vehicle guidance on the motorway. In *Proceedings of the IEEE Intelligent Vehicles Symposium, Paris, France*, 1994.

[5] D. Reichardt. Kontinuierliche Verhaltenssteuerung eines autonomen Fahrzeugs in dynamischer Umgebung. PhD thesis, Fachbereich Informatik der Universitaet Kaiserslautern, May 1996.

[6] M. Hennessey, C. Shankwitz, and M. Donath. Sensor based 'virtual bumpers' for collision avoidance: Configuration issues. In *Proceedings of the SPIE*, volume 2592, 1995.

[7] B. Schiller, V. Morellas, and M. Donath. Collision avoidance for highway vehicles using the virtual bumper controller. In *Proceedings of the 1998 IEEE International Symposium on Intelligent Vehicles, Stuttgart, Germany*, October 1998.

[8] B. Schiller, Y. Du, D. Krantz, C. Shankwitz, and M. Donath. *Vehicle Guidance Architecture for Combined Lane Tracking and Obstacle Avoidance*, chapter 7 in Artifical Intelligence and Mobile Robots: Case Studies of Successful Robot Systems, pages 159–192. AIII Press/The MIT Press, Cambridge, MA, 1998.

[9] B. Koepele and J. Starkey. Closed-loop vehicle and driver models for high-speed trajectory following. In *Transportation Systems - 1990 ASME WAM, Dallas, TX*, pages 59–68, 1990.

[10] C. Chen and M. Tomizuka. Passivity-based nonlinear observer for lateral control of tractor-trailer vehicles in automated highway systems. In *Proceedings of the 1996 IFAC, San Francisco, CA*, pages 273–278, 1996.

[11] J.C. Gerdes and E.J. Rossetter. A unified approach to driver assistance systems based on artificial potential fields. In *Proceedings of the 1999 ASME IMECE, Nashville, TN*, 1999.

[12] R. Guntur and S. Sankar. A friction circle concept for dugoff's tyre friction model. *International Journal of Vehicle Design*, 4(1):373–377, 1980.

[13] C.K.H. Wilson, S. Rogers, and S. Weisenburger. The potential of precision maps in intelligent vehicles. In *Proceedings of the IEEE Intelligent Transportation Systems Conference, Stuttgart, Germany*, 1998.

[14] S. Gehrig and F. Stein. Trajectory-based approach for the lateral control of car following systems. In *Proceedings of the IEEE International Conference on Systems, Man and Cybernetics*, 1998.

[15] V. Alberti and E. Babbel. Improved driving stability by active braking of the individual wheels. In *Proceedings of AVEC 96, Aachen University of Technology, June, 1996*, pages 717–732, 1996.

[16] R.J. Cooke, D.A. Crolla, and M. Abe. Combined ride and handling modelling of a vehicle with active suspension. In *Proceedings of AVEC 96, Aachen University of Technology, June, 1996*, pages 1037–1053, 1996.

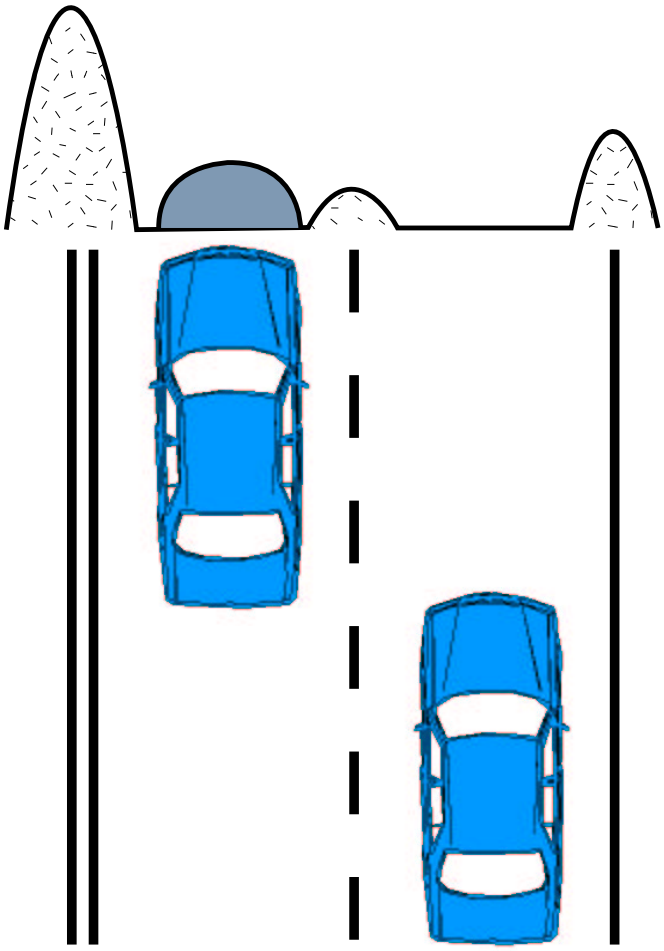

Figure 1: Cross Section of Potential Function

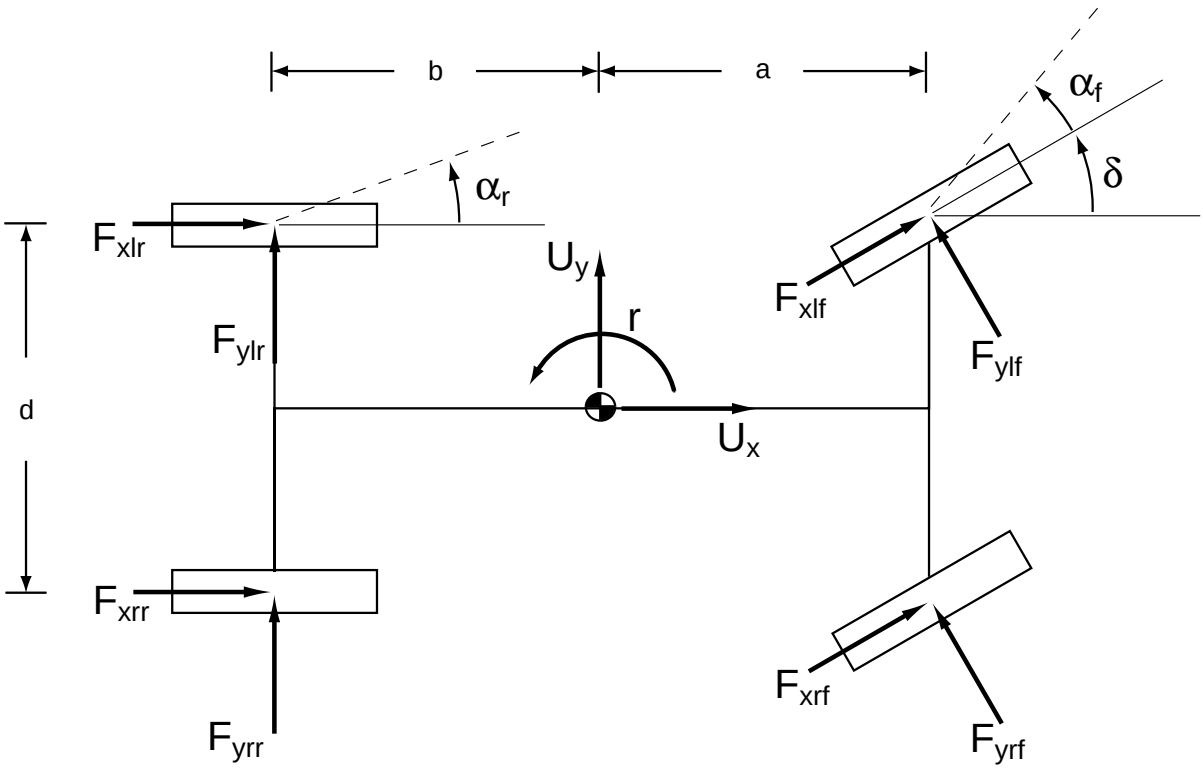

Figure 2: Planar Model of Vehicle Dynamics

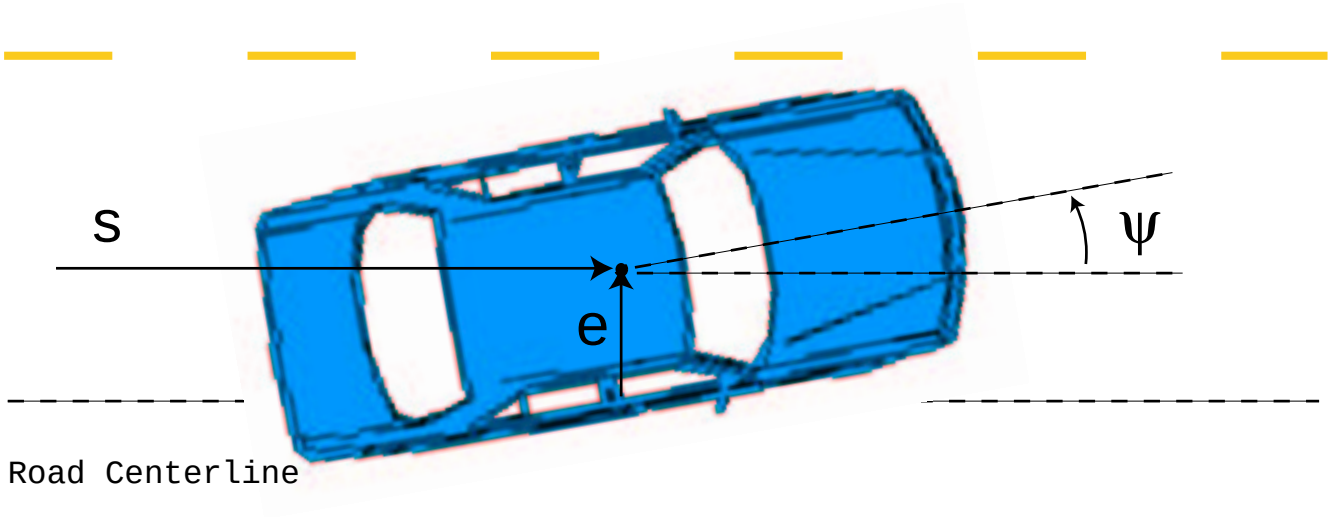

Figure 3: Global Coordinates

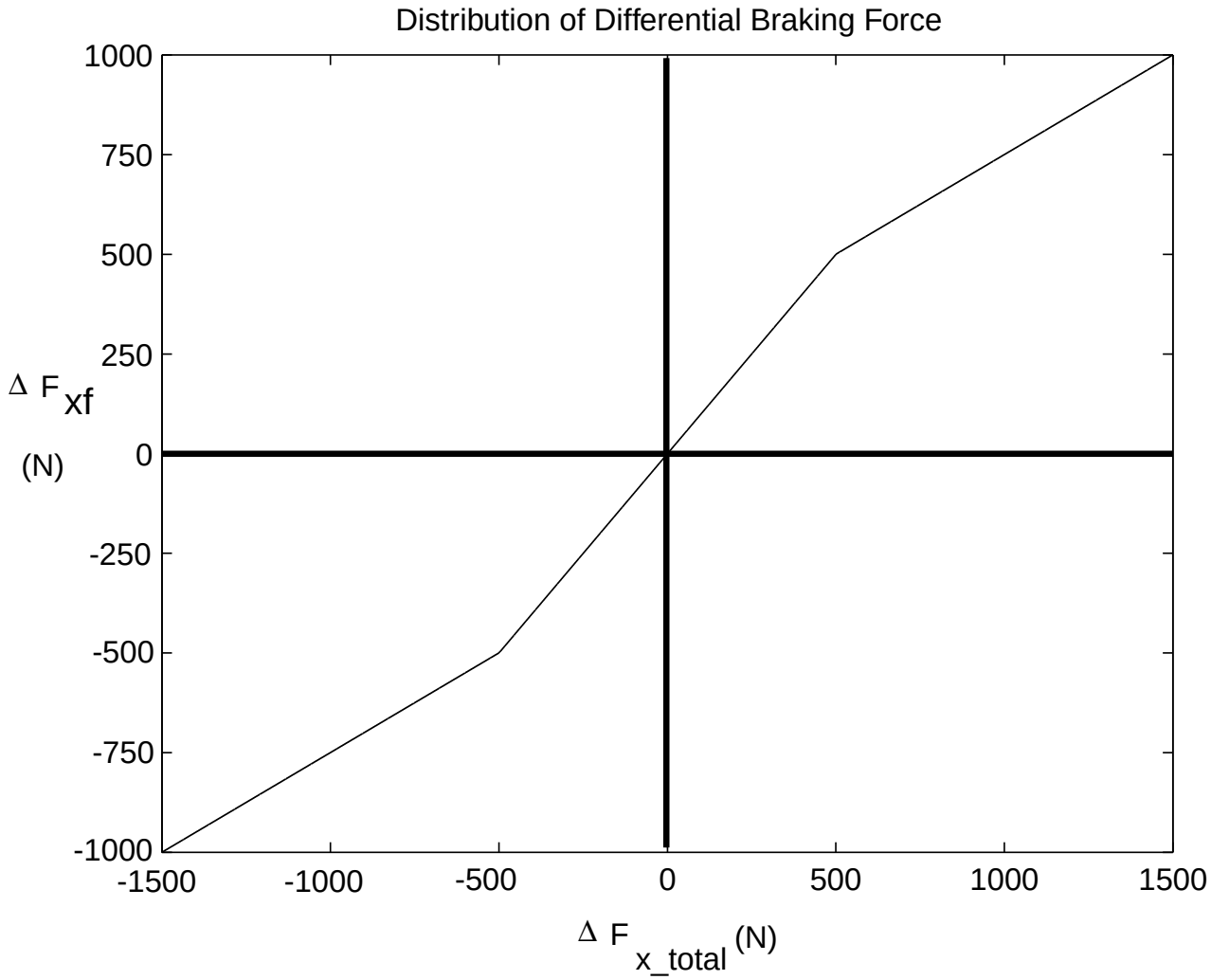

Figure 4: Differential Braking Distribution

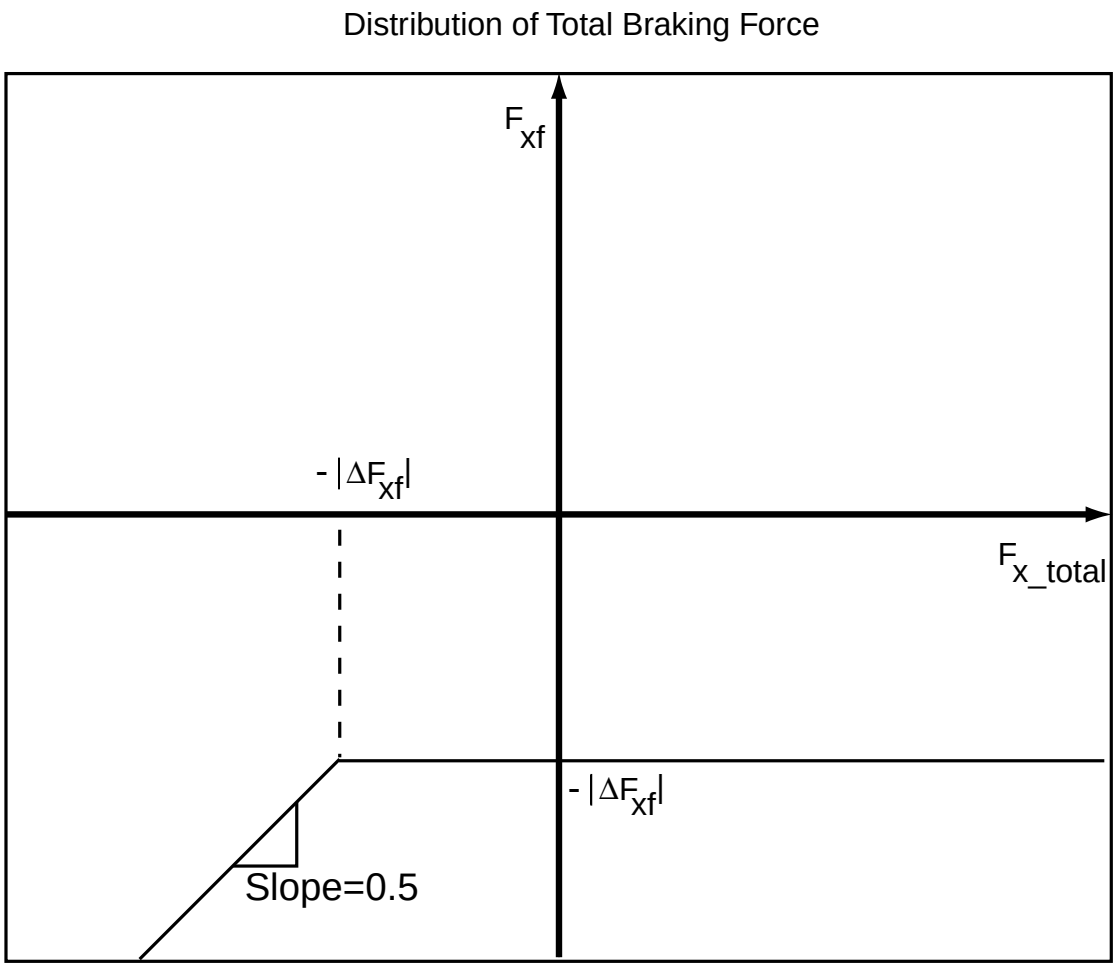

Figure 5: Front/Rear Brake Distribution

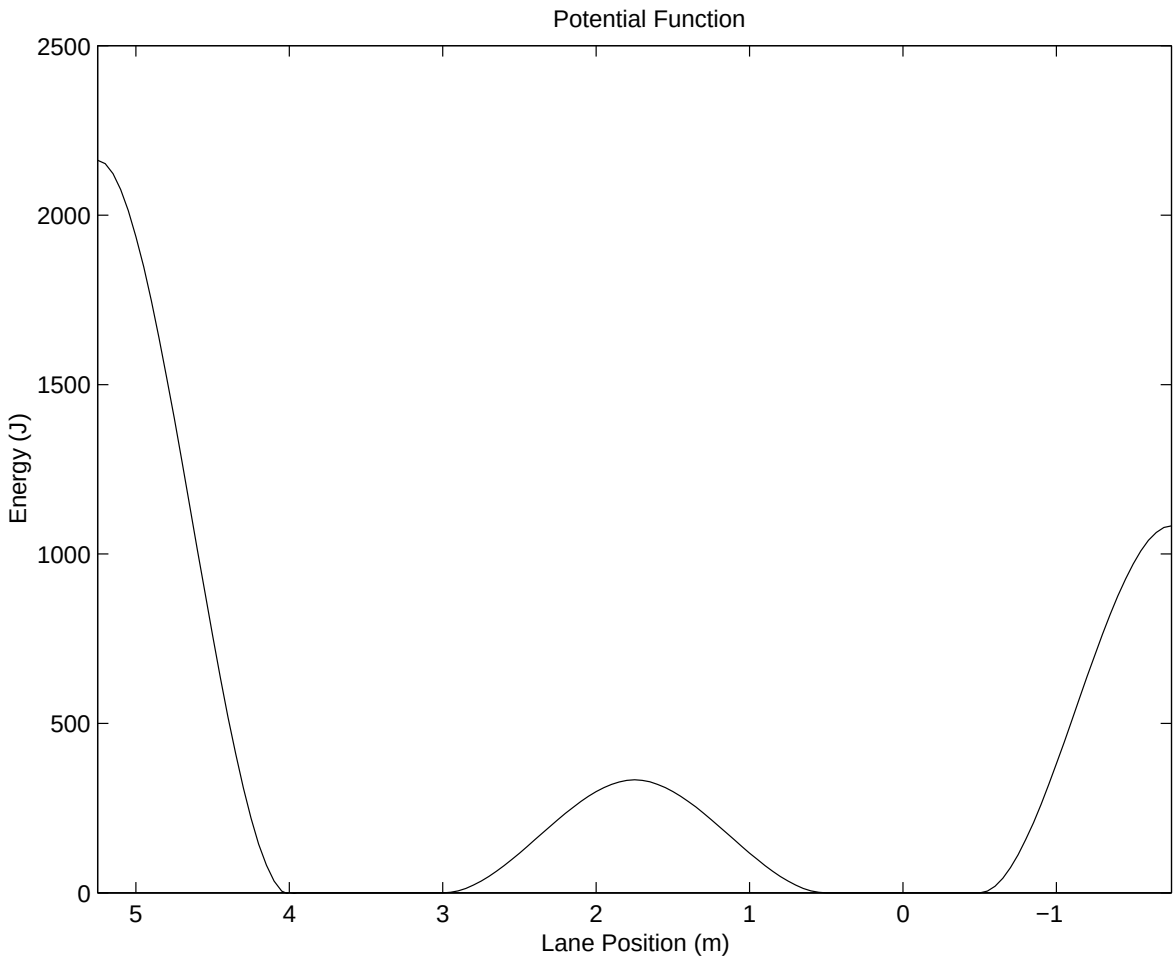

Figure 6: Section of Lanekeeping Potential Function

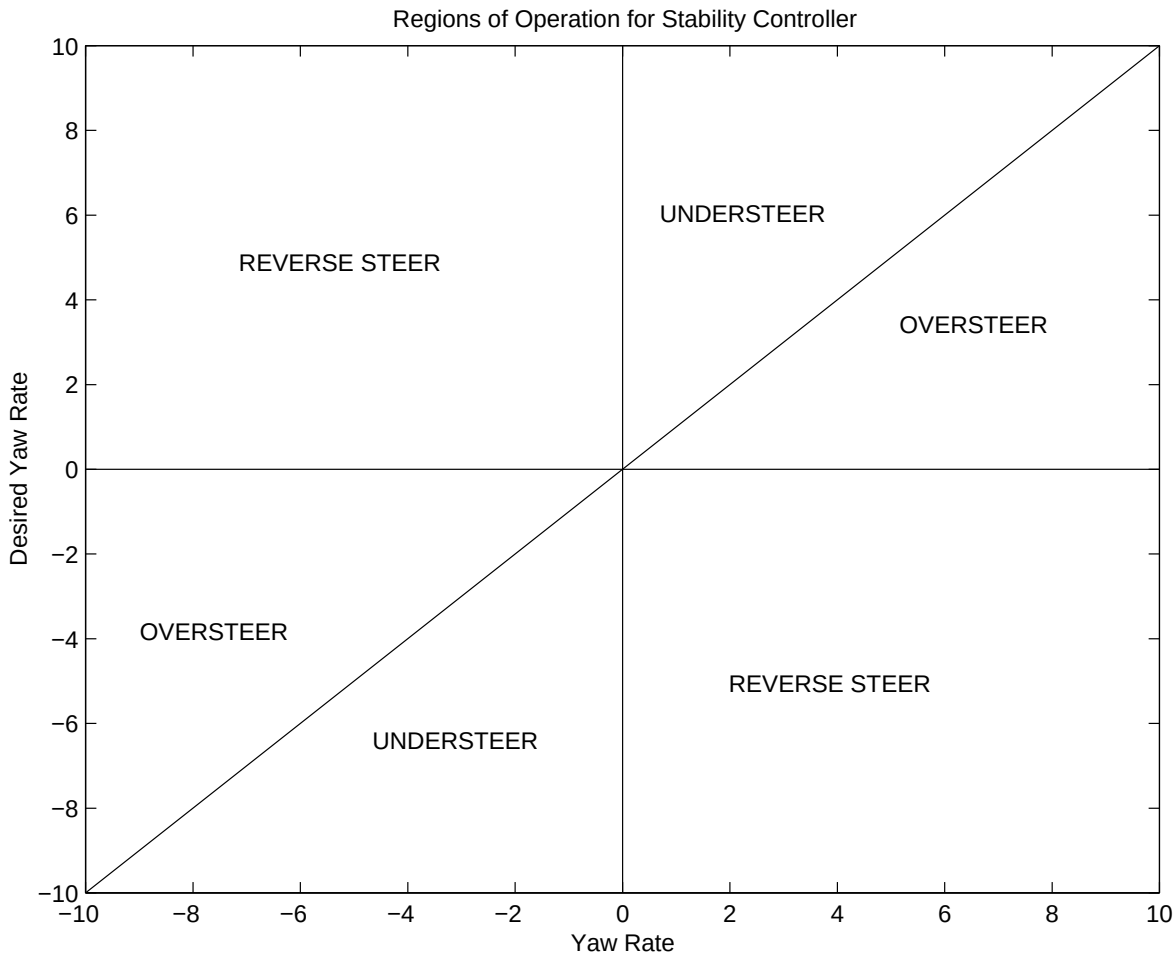

Figure 7: Stability Control Regions of Operation

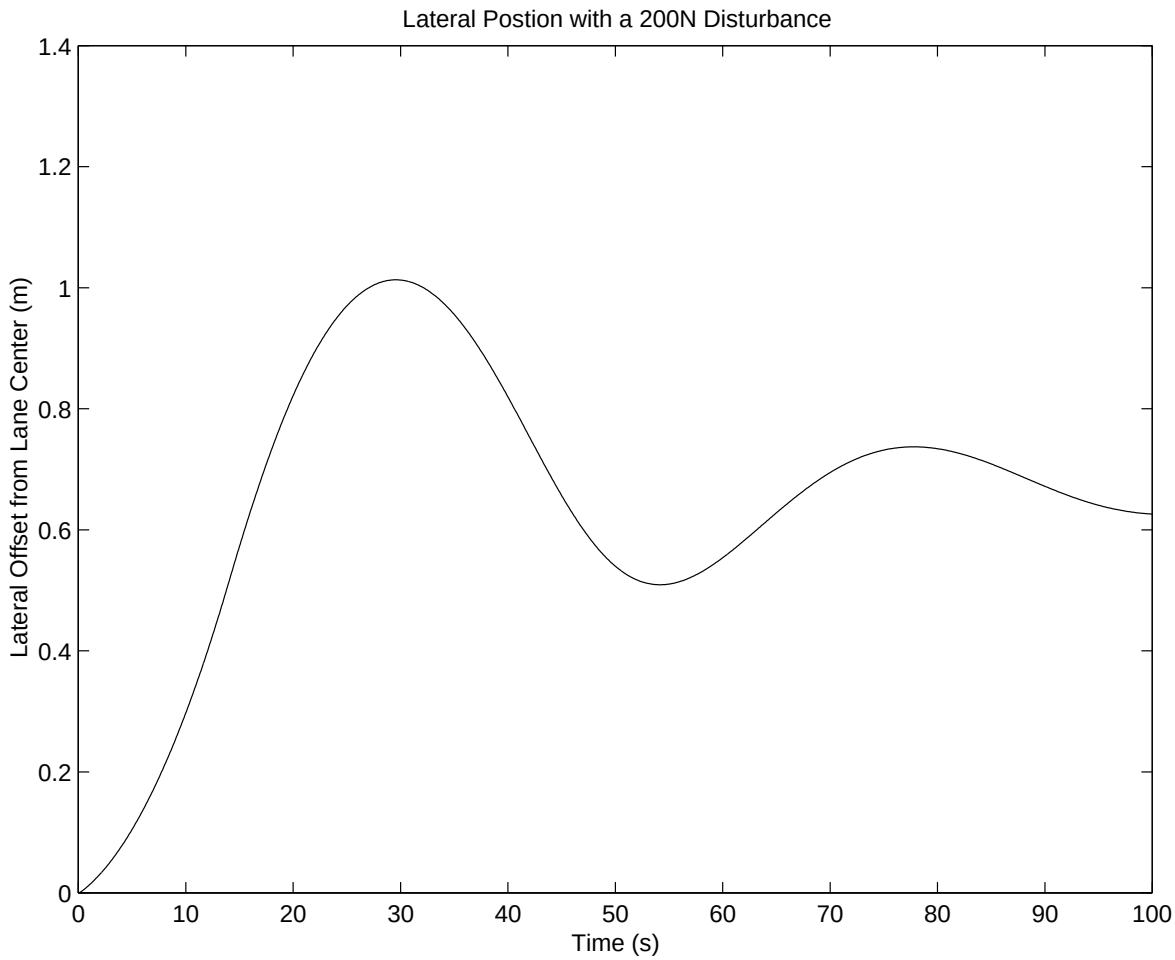

Figure 8: Response with Lateral Disturbance

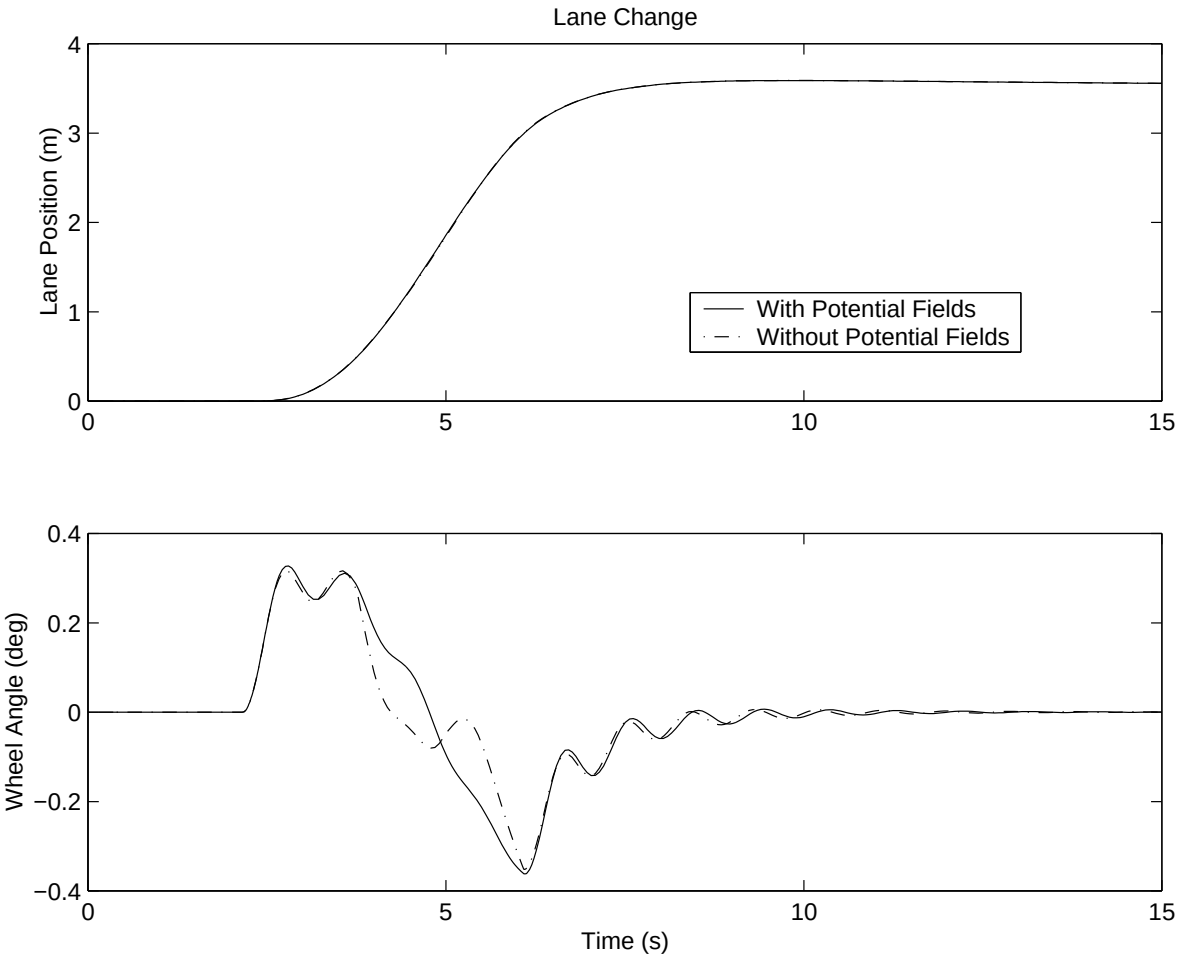

Figure 9: Gentle Lane Change Response

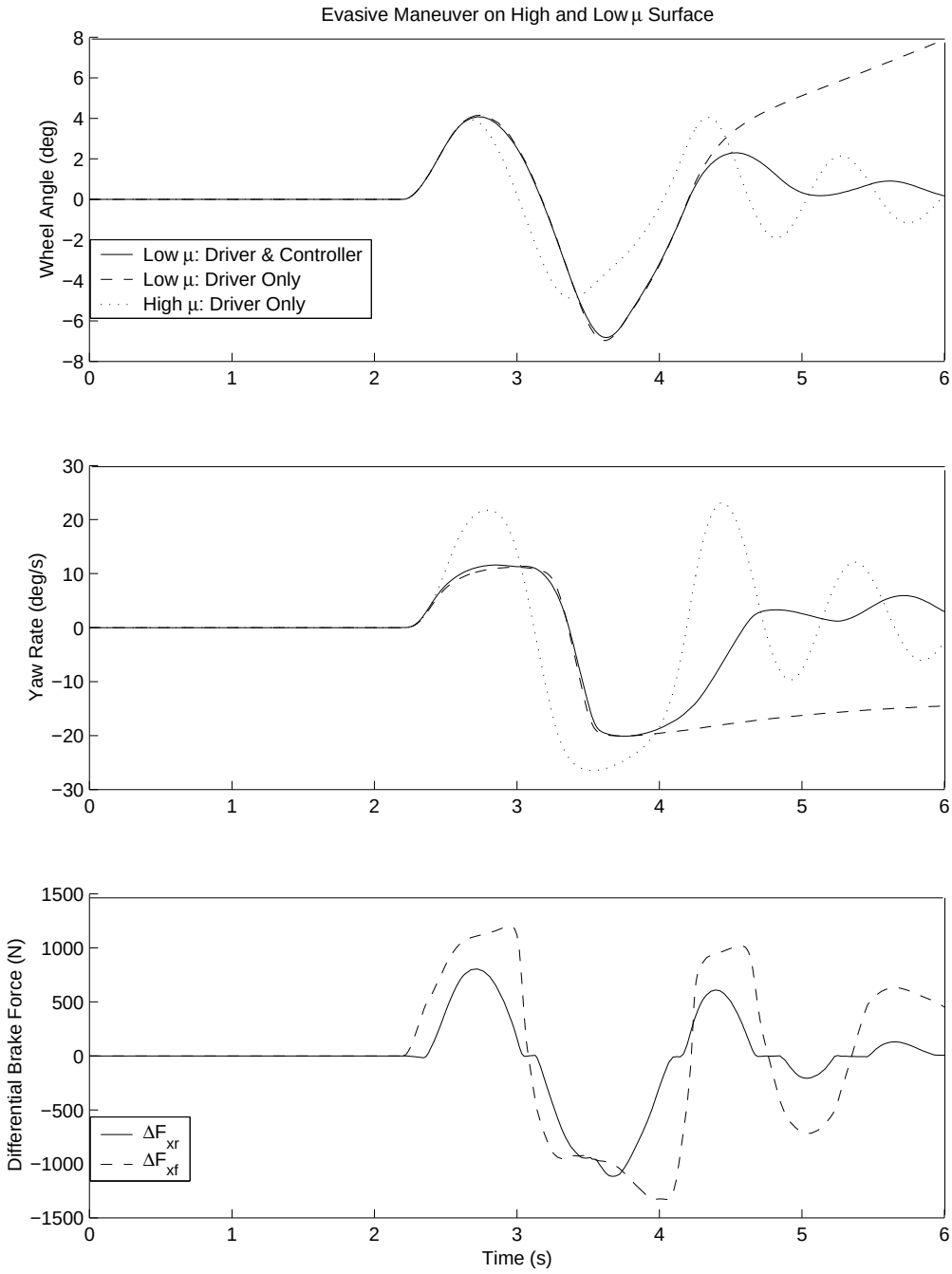

Figure 10: Avoidance Maneuver Response